

UC Santa Cruz

UC Santa Cruz Previously Published Works

Title

Riemann-Stieltjes optimal control problems for uncertain dynamic systems

Permalink

<https://escholarship.org/uc/item/4jq3s10x>

Journal

Journal of Guidance, Control, and Dynamics, 38(7)

ISSN

0731-5090

Authors

Ross, IM
Proulx, RJ
Karpenko, M
et al.

Publication Date

2015

DOI

10.2514/1.G000505

Peer reviewed

Riemann–Stieltjes Optimal Control Problems for Uncertain Dynamic Systems

I. Michael Ross,^{*} Ronald J. Proulx,[†] and Mark Karpenko[‡]
Naval Postgraduate School, Monterey, California 93943
 and
 Qi Gong[§]
University of California, Santa Cruz, California 95064

DOI: 10.2514/1.G000505

Motivated by uncertain parameters in nonlinear dynamic systems, we define a nonclassical optimal control problem where the cost functional is given by a Riemann–Stieltjes “functional of a functional.” Using the properties of Riemann–Stieltjes sums, a minimum principle is generated from the limit of a semidiscretization. The optimal control minimizes a Riemann–Stieltjes integral of the Pontryagin Hamiltonian. The challenges associated with addressing the noncommutative operations of integration and minimization are addressed via cubature techniques leading to the concept of hyper-pseudospectral points. These ideas are then applied to address the practical uncertainties in control moment gyroscopes that drive an agile spacecraft. Ground test results conducted at Honeywell demonstrate the new principles. The Riemann–Stieltjes optimal control problem is a generalization of the unscented optimal control problem. It can be connected to many independently developed ideas across several disciplines: search theory, viability theory, quantum control and many other applications involving tyochastic differential equations.

I. Introduction

WE CONSIDER uncertain dynamic systems parameterized by

$$\dot{\mathbf{x}} = \mathbf{f}(\mathbf{x}, \mathbf{u}, t; \mathbf{p}) \quad (1)$$

where $\mathbf{x} \in \mathbb{R}^{N_x}$ is the state variable, $\mathbf{u} \in \mathbb{R}^{N_u}$ is the control variable, $t \in \mathbb{R}$ is the time variable, and $\mathbf{p} \in \mathbb{R}^{N_p}$ is an uncertain parameter such that the function $\mathbf{f}: (\mathbf{x}, \mathbf{u}, t; \mathbf{p}) \mapsto \mathbb{R}^{N_x}$ is deterministic if \mathbf{p} is known. Such dynamic systems are standard fare in aerospace and marine engineering. Examples are unmanned aerial vehicles, trans-atmospheric launch and reentry vehicles, space vehicles, missiles, surface vehicles, and underwater vehicles. The uncertain parameters in these examples arise from endogenous uncertainties such as lift, drag, and moment coefficients, moments and cross products of inertia, control alignment parameters, etc. Exogenous uncertainties such as unknowns in the environment (e.g., air or water density) are also naturally included in \mathbf{p} .

Now, suppose we pick a specific value \mathbf{p}_1^* of the uncertain parameter \mathbf{p} and construct a feasible system trajectory, that transfers the deterministic dynamic system

$$\dot{\mathbf{x}} = \mathbf{f}(\mathbf{x}, \mathbf{u}, t; \mathbf{p}_1^*) \quad (2)$$

from a given initial point \mathbf{x}^0 to a specified final point \mathbf{x}^f , as illustrated in Fig. 1. Denote this feasible system trajectory as $(\mathbf{x}^1(\cdot), \mathbf{u}^1(\cdot))$. If we now apply the open-loop control $t \mapsto \mathbf{u}^1$ to the uncertain dynamic system [given by Eq. (1)], then the resulting state trajectory $\mathbf{x}^1(\cdot, \mathbf{p})$ will, in general, not be the same as $\mathbf{x}^1(\cdot)$, as illustrated in Fig. 1, unless of course, $\mathbf{p} = \mathbf{p}_1^*$ by chance. Now, suppose we repeat the preceding

exercise for $\mathbf{p} = \mathbf{p}_2^*$; that is, we produce a feasible system trajectory, $(\mathbf{x}^2(\cdot), \mathbf{u}^2(\cdot))$ for the deterministic system

$$\dot{\mathbf{x}} = \mathbf{f}(\mathbf{x}, \mathbf{u}, t; \mathbf{p}_2^*) \quad (3)$$

and apply the open-loop control $t \mapsto \mathbf{u}^2$ to the uncertain dynamic system $\dot{\mathbf{x}} = \mathbf{f}(\mathbf{x}, \mathbf{u}, t; \mathbf{p})$ and generate a state trajectory $\mathbf{x}^2(\cdot, \mathbf{p})$, as illustrated in Fig. 2. Qualitatively, the result of this exercise will be same as before; however, it will, in general, differ quantitatively from the previous one. Now, suppose that this quantitative difference is such that $\mathbf{x}^2(t_f, \mathbf{p})$ is closer to \mathbf{x}^f than $\mathbf{x}^1(t_f, \mathbf{p})$ in some desired metric “dist”; that is, suppose that

$$\text{dist}(\mathbf{x}^2(t_f, \mathbf{p}), \mathbf{x}^f) < \text{dist}(\mathbf{x}^1(t_f, \mathbf{p}), \mathbf{x}^f) \quad (4)$$

Then, we can argue that $\mathbf{x}^2(\cdot, \mathbf{p})$ is a better trajectory than $\mathbf{x}^1(\cdot, \mathbf{p})$ because it is closer to the goal point \mathbf{x}^f . This argument then generates the question: What is the best trajectory? In framing this question more precisely, we need to mathematically articulate the meaning of the word “best” that properly accounts for the fact that \mathbf{p} is an uncertain parameter. That is, we need to define a cost functional whose minimum can be described as best. To this end, we propose a multidimensional Riemann–Stieltjes integral [1,2] as the objective functional

$$\int \dots \int \|\mathbf{x}(t_f, \mathbf{p}) - \mathbf{x}^f\| d\alpha'(\mathbf{p}) \quad (5)$$

where $\|\cdot\|$ is some appropriate norm that serves the role of a metric, and

$$\alpha': \mathbf{p} \mapsto \mathbb{R} \quad (6)$$

is a given joint cumulative distribution function (CDF) of \mathbf{p} . It is clear that Eq. (5) is not a cost functional that is commonly encountered in standard optimal control. In fact, even in the special case of $N_p = 1$, when the multidimensional integral can be reduced to a definite one-dimensional integral,

$$\int_{p_1}^{p_2} \|\mathbf{x}(t_f, p) - \mathbf{x}^f\| d\alpha'(p) \quad (7)$$

where $[p_1, p_2]$ is the domain of p , the cost functional is not standard, that is, Lagrange type [3], because the integral is not over time but

Received 10 January 2014; revision received 15 July 2014; accepted for publication 22 July 2014; published online 10 February 2015. Copyright © 2014 by Isaac M. Ross, Ronald J. Proulx, and Mark Karpenko. Published by the American Institute of Aeronautics and Astronautics, Inc., with permission. Copies of this paper may be made for personal or internal use, on condition that the copier pay the \$10.00 per-copy fee to the Copyright Clearance Center, Inc., 222 Rosewood Drive, Danvers, MA 01923; include the code 1533-3884/15 and \$10.00 in correspondence with the CCC.

^{*}Professor and Program Director, Control and Optimization.

[†]Professor of Practice, Control and Optimization.

[‡]Research Assistant Professor, Control and Optimization; mkarpenk@nps.edu (Corresponding Author).

[§]Associate Professor, Department of Applied Mathematics and Statistics.

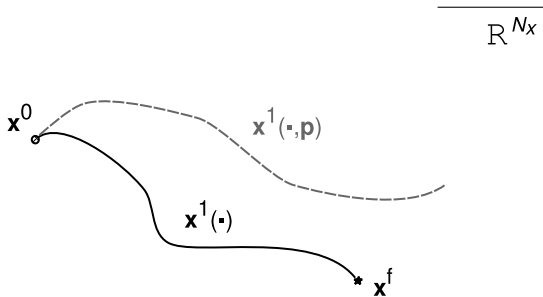


Fig. 1 Illustration of one possible effect of the feasible control trajectory $t \mapsto \mathbf{u}^1$ on the uncertain dynamic system $\dot{\mathbf{x}} = \mathbf{f}(\mathbf{x}, \mathbf{u}^1(t), t; \mathbf{p})$ for $\mathbf{p} \neq \mathbf{p}_1^*$.

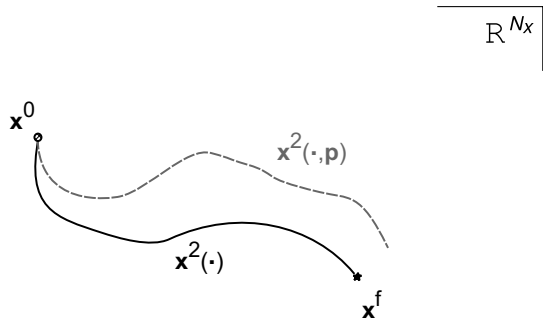


Fig. 2 Illustration of the effect of a feasible control trajectory $t \mapsto \mathbf{u}^2$ that is of superior performance to Fig. 1 when the performance index is given by Eq. (4).

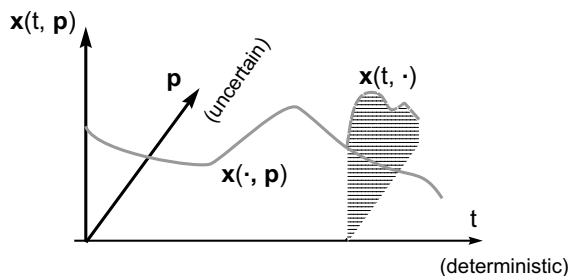


Fig. 3 Schematic of a sample of some key functions used in defining a Riemann–Stieltjes optimal control problem.

over the space of p . Note also that our concept is not limited to a finite domain of integration; in fact, the infinite line $(-\infty, \infty)$ is an important domain for many CDFs such as a Gaussian distribution. Thus, Eq. (5) is not a cost functional encountered in standard optimal control. In this paper, we generalize the concept embedded in Eq. (5) to a nonlinear functional of a functional and frame a new mathematical problem formulation.

Before proceeding further, we note that we have implicitly used the notation $\mathbf{x}(t, \mathbf{p})$ to describe a solution to the parameterized initial-value problem

$$\dot{\mathbf{x}} = \mathbf{g}(\mathbf{x}, t; \mathbf{p}) \quad \text{with} \quad \mathbf{x}(t_0, \mathbf{p}) = \mathbf{x}^0$$

where $\mathbf{g}(\mathbf{x}, t; \mathbf{p}) := \mathbf{f}(\mathbf{x}, \mathbf{u}(t), t; \mathbf{p})$. In the mathematics to follow, it will also be useful to denote a particular trajectory for a given value of \mathbf{p} by $\mathbf{x}(\cdot, \mathbf{p})$, and a slice of trajectories at t by $\mathbf{x}(t, \cdot)$ (see Fig. 3). More formally, we define

$$\mathbf{x}(\cdot, \mathbf{p}): t \mapsto \mathbb{R}^{N_x} \quad \mathbf{x}(t, \cdot): \mathbf{p} \mapsto \mathbb{R}^{N_x} \quad \mathbf{x}(\cdot, \cdot): (t, \mathbf{p}) \mapsto \mathbb{R}^{N_x} \quad (8)$$

Note, therefore, that $\mathbf{x}(\cdot, \mathbf{p})$, $\mathbf{x}(t, \cdot)$, and $\mathbf{x}(\cdot, \cdot)$ are all completely different functions despite the fact that we have used a common notation \mathbf{x} as part of the symbols that define these different functions. We use this commonality for the convenience of signifying that all these different functions take (different) values in the common

“range” space, namely, $\mathbb{X} = \mathbb{R}^{N_x}$. In the discussions to follow, it will also be apparent that all these functions are elements of different function spaces as well. In this context, we will make all of the typical assumptions of standard optimal control [4,5]; hence, we assume $\mathbf{x}(\cdot, \mathbf{p}) \in W^{1,1}$ for each \mathbf{p} and $\mathbf{u}(\cdot) \in L^\infty$, where $W^{1,1}$ is the space of absolutely continuous functions and L^∞ is the space of bounded functions with $\mathbf{u}(t)$ taking values in a compact set $\mathbb{U} \subseteq \mathbb{R}^{N_u}$ for each t . Strictly speaking, L^∞ is the space of essentially bounded measurable functions; however, except for mathematical clarity, we will not employ such language or rigor in favor of sufficient engineering mathematics that outline the basic abstractions. This is why we call Eq. (5) a Riemann–Stieltjes integral and not a Lebesgue–Stieltjes integral [1]. In this spirit, we also use Riemann sums in Sec. IV, and assume that $\mathbf{x}(t, \cdot) \in L^1$ for each t where L^1 is the space of integrable functions.

II. Development of a Preliminary Mathematical Problem Formulation

Consider the dynamic system given by Eq. (1). In addition to uncertainties in \mathbf{p} , we allow the system to have uncertainties in its initial values of the state vector \mathbf{x}^0 , as well as the clock time t^0 . This implies that we will consider the triple t^0 , \mathbf{x}^0 , and \mathbf{p} to be uncertain variables. For theoretical expedience, we transform the system to the following “extended” dynamic system

$$\begin{cases} \dot{\mathbf{x}} = \mathbf{f}(\mathbf{x}, \mathbf{u}, s; \mathbf{p}) \\ \dot{\mathbf{p}} = 0 \\ \dot{s} = 1 \end{cases} \quad (9)$$

so that all the uncertainties can be mapped to those in the initial conditions only. Hence, it suffices to consider the autonomous dynamic system

$$\dot{\mathbf{x}} = \mathbf{f}(\mathbf{x}, \mathbf{u}) \quad (10)$$

with uncertainties in the initial condition \mathbf{x}^0 only. Consequently, we replace \mathbf{p} in Eq. (8) by \mathbf{x}^0 and use the symbol $\mathbf{x}(t, \mathbf{x}^0)$ without loss of generality.

Now suppose that, for a fixed value of \mathbf{x}^0 , we are given a standard deterministic cost functional J_{std} ,

$$J_{\text{std}}[\mathbf{x}(\cdot), \mathbf{u}(\cdot)] \quad (11)$$

Thus, J_{std} is some standard cost functional [4,6] $J_{\text{std}}: W^{1,1} \times L^\infty \rightarrow \mathbb{R}$. Given such a cost functional for every \mathbf{x}^0 , we can conceive of an abstract map

$$\mathbf{x}^0 \mapsto J_{\text{std}}$$

that produces a formula for any given value of \mathbf{x}^0 . In this spirit, we define J_{unc} as a functional which allows the uncertain parameter \mathbf{x}^0 as part of its input

$$J_{\text{unc}}[\mathbf{x}(\cdot, \mathbf{x}^0), \mathbf{u}(\cdot); \mathbf{x}^0] \quad (12)$$

Thus, for any given value of \mathbf{x}^0 , J_{unc} is possibly the same formula as J_{std} with $\mathbf{x}(\cdot)$ replaced by $\mathbf{x}(\cdot, \mathbf{x}^0)$ (for a fixed \mathbf{x}^0). In this sense, we have somewhat abused the notation $\mathbf{x}(\cdot, \mathbf{x}^0)$ in Eq. (12) to imply the map $\mathbf{x}^0 \mapsto \mathbf{x}(\cdot, \mathbf{x}^0)$. Additionally, J_{unc} allows new terms in its formulation through its explicit dependence on \mathbf{x}^0 facilitated through its last argument. An important difference between these two cost functionals is that, in J_{std} , all of its arguments are decision variables, whereas in J_{unc} , \mathbf{x}^0 is an uncertain argument [of J_{unc} and $\mathbf{x}(\cdot, \cdot)$] but is not a decision variable. Thus, J_{unc} generates the real-valued function

$$\mathbf{x}^0 \mapsto J_{\text{unc}}[\mathbf{x}(\cdot, \mathbf{x}^0), \mathbf{u}(\cdot); \mathbf{x}^0] \in \mathbb{R} \quad (13)$$

via a functional. Motivated by Eq. (5), we use the function given by Eq. (13) to define a Riemann–Stieltjes J functional as a functional of a functional, given by

$$J[\mathbf{x}(\cdot, \cdot), \mathbf{u}(\cdot)] := \int_{\text{supp}(\mathbf{x}^0)} J_{\text{unc}}[\mathbf{x}(\cdot, \mathbf{x}^0), \mathbf{u}(\cdot); \mathbf{x}^0] d\alpha''(\mathbf{x}^0) \quad (14)$$

where α'' is the joint CDF of \mathbf{x}^0 , $\text{supp}(\mathbf{x}^0)$ denotes the support of \mathbf{x}^0 , and

$$\int_{\text{supp}(\mathbf{x}^0)}$$

is a shorthand notation for the multiple integral

$$\int \cdots \int_{\text{supp}(\mathbf{x}^0)} \quad (15)$$

In subsequent sections, it will be useful to interpret the first argument of J as a state trajectory tube [7] $\{t \mapsto \mathbf{x}(t, \mathbf{x}^0): \mathbf{x}^0 \in \text{supp}(\mathbf{x}^0)\}$, whereas its second argument is a single control trajectory $\mathbf{u}(\cdot)$. Thus, we can now define a preliminary Riemann–Stieltjes optimal control problem as the problem to determine the conditionally deterministic decision pair $(\mathbf{x}(\cdot, \cdot), \mathbf{u}(\cdot))$, which minimizes the J functional subject to the dynamic constraint given by Eq. (10).

To further this initial problem formulation, it is necessary to stipulate generic boundary conditions. Given that \mathbf{x}^0 is an uncertain parameter, the simplest formulation is to set $\boldsymbol{\mu}_{\mathbf{x}^0}$ to some fixed value, where $\boldsymbol{\mu}_{\mathbf{x}^0}$ is the mean of \mathbf{x}^0 . Such a formulation is used in [8,9] in one instantiation of a Riemann–Stieltjes formulation called unscented optimal control. Generalizing along this direction, we may set $\boldsymbol{\mu}_{\mathbf{x}^0}$ to be a decision variable that must be selected from some given set $\mathbb{X}_{\boldsymbol{\mu}}^0 \subseteq \mathbb{R}^{N_x}$. By analogy, the same arguments hold for the final time conditions as well, that is, to allow $\boldsymbol{\mu}_{\mathbf{x}^f}$ to be a decision variable selectable from some given set $\mathbb{X}_{\boldsymbol{\mu}}^f \subseteq \mathbb{R}^{N_x}$. Generalizing this notion further, we let \mathbf{r} be the uncertain parameter defined by

$$\mathbf{r} := \begin{bmatrix} \mathbf{x}^0 \\ \mathbf{x}^f \end{bmatrix} \quad (16)$$

and stipulate that $\text{supp}(\mathbf{r})$ be equal to some given set that may be chosen as a subset of an endpoint set $\mathbb{E} \subseteq \mathbb{X} \times \mathbb{X}$. Practical examples of such requirements are discussed in [8,9]. In accounting for the entire collection of uncertain parameters, we generalize the Riemann–Stieltjes J functional to

$$J[\mathbf{x}(\cdot, \cdot), \mathbf{u}(\cdot)] := \int_{\text{supp}(\mathbf{r})} J_{\text{unc}}[\mathbf{x}(\cdot, \mathbf{r}), \mathbf{u}(\cdot); \mathbf{r}] d\alpha(\mathbf{r}) \quad (17)$$

where $\alpha: \mathbf{r} \mapsto \mathbb{R}$ is the joint CDF of \mathbf{r} . Note that, by virtue of Eq. (9), our problem formulation includes uncertainties in the final time as well.

III. Fundamental Riemann–Stieltjes Optimal Control Problem Formulation

Suppose that a standard cost functional is given in the form of an integral (i.e., a “Lagrange form”)

$$J_{\text{std}}[\mathbf{x}(\cdot), \mathbf{u}(\cdot)] := \int_{t_0}^{t_f} F(\mathbf{x}(t), \mathbf{u}(t)) dt$$

where $F: \mathbb{R}^{N_x} \times \mathbb{R}^{N_u} \rightarrow \mathbb{R}$ is some given data function. Then, replacing $\mathbf{x}(t)$ by $\mathbf{x}(t, \mathbf{r})$, we can generate the map $\mathbf{r} \mapsto J_{\text{unc}}$ from

$$J_{\text{unc}}[\mathbf{x}(\cdot, \mathbf{r}), \mathbf{u}(\cdot)] := \int_{t_0}^{t_f} F(\mathbf{x}(t, \mathbf{r}), \mathbf{u}(t)) dt \quad (18)$$

Using Eq. (17) as the framework, we can formulate a Riemann–Stieltjes J functional as

$$\begin{aligned} J[\mathbf{x}(\cdot, \cdot), \mathbf{u}(\cdot)] &:= \int_{\text{supp}(\mathbf{r})} J_{\text{unc}}[\mathbf{x}(\cdot, \mathbf{r}), \mathbf{u}(\cdot)] d\alpha(\mathbf{r}) \\ &= \int_{\text{supp}(\mathbf{r})} \left(\int_{t_0}^{t_f} F(\mathbf{x}(t, \mathbf{r}), \mathbf{u}(t)) dt \right) d\alpha(\mathbf{r}) \end{aligned} \quad (19)$$

This equation reaffirms the notion that the J functional is a nonlinear functional of a functional. Now, let $z: (t, \mathbf{r}) \mapsto \mathbb{R}$ be a function, such that

$$\dot{z}(t, \mathbf{r}) := F(\mathbf{x}(t, \mathbf{r}), \mathbf{u}(t)) \quad (20)$$

Then, it follows that

$$\int_{t_0}^{t_f} F(\mathbf{x}(t, \mathbf{r}), \mathbf{u}(t)) dt = z(t_f, \mathbf{r}) - z(t_0, \mathbf{r})$$

Hence Eq. (19) can be transformed to

$$J[\mathbf{x}(\cdot, \cdot), \mathbf{u}(\cdot)] = \int_{\text{supp}(\mathbf{r})} (z(t_f, \mathbf{r}) - z(t_0, \mathbf{r})) d\alpha(\mathbf{r}) \quad (21)$$

with the understanding that Eq. (20) is now part of the extended dynamics given by Eq. (9). Noting that the integrand in Eq. (21) is a function of the endpoints only, we can generalize the representation of the J functional to

$$J[\mathbf{x}(\cdot, \cdot), \mathbf{u}(\cdot)] = \int_{\text{supp}(\mathbf{r})} E(\mathbf{r}) d\alpha(\mathbf{r}) \quad (22)$$

where $E: \mathbf{r} \mapsto \mathbb{R}$. Thus, if a standard cost functional were given in an endpoint form (i.e., a “Mayer” form) [3,6],

$$J_{\text{std}}[\mathbf{x}(\cdot), \mathbf{u}(\cdot)] := E(\mathbf{x}^0, \mathbf{x}^f) \quad (23)$$

where $E: \mathbb{R}^{N_x} \times \mathbb{R}^{N_x} \rightarrow \mathbb{R}$, it is apparent that we can generate a Riemann–Stieltjes cost functional by quite simply integrating the endpoint function E using the CDF α as the integrator. Thus, we can now define a fundamental Riemann–Stieltjes (RS) optimal control problem as follows:

$$\begin{aligned} \mathbf{x}(t, \mathbf{r}) &\in \mathbb{X} = \mathbb{R}^{N_x}, & \mathbf{u}(t) &\in \mathbb{U} \subset \mathbb{R}^{N_u} \\ \mathbf{r} &:= (\mathbf{x}^0, \mathbf{x}^f) \in \text{supp}(\mathbf{r}) \subset \mathbb{X} \times \mathbb{X} \end{aligned} \quad (RS) \begin{cases} \text{Minimize} & J[\mathbf{x}(\cdot, \cdot), \mathbf{u}(\cdot)] = \int_{\text{supp}(\mathbf{r})} E(\mathbf{r}) d\alpha(\mathbf{r}) \\ \text{Subject to} & \dot{\mathbf{x}}(t, \mathbf{r}) = \mathbf{f}(\mathbf{x}(t, \mathbf{r}), \mathbf{u}(t)) \\ & \int_{\text{supp}(\mathbf{r})} \mathbf{e}(\mathbf{r}) d\alpha(\mathbf{r}) \leq 0 \end{cases} \quad (24)$$

where $\mathbf{e}: \mathbf{r} \mapsto \mathbb{R}^{N_e}$ is some given data function that constrains the endpoints via an inequality of a vector integral.

IV. Development of the Necessary Conditions

We define an adjoint covector function $t \mapsto \boldsymbol{\lambda}(t, \mathbf{r}) \in \mathbb{R}^{N_x}$ for each \mathbf{r} , as the solution to the adjoint differential equation

$$-\dot{\boldsymbol{\lambda}} = \partial_{\mathbf{x}} H(\boldsymbol{\lambda}, \mathbf{x}(t, \mathbf{r}), \mathbf{u}(t)) \quad (25)$$

where H is the Pontryagin Hamiltonian function

$$H(\boldsymbol{\lambda}, \mathbf{x}, \mathbf{u}) := \boldsymbol{\lambda}^T \mathbf{f}(\mathbf{x}, \mathbf{u})$$

It will be apparent shortly that the integral of the Hamiltonian

$$I[\boldsymbol{\lambda}(t, \cdot), \mathbf{x}(t, \cdot), \mathbf{u}] := \int_{\text{supp}(\mathbf{r})} H(\boldsymbol{\lambda}(t, \mathbf{r}), \mathbf{x}(t, \mathbf{r}), \mathbf{u}) d\alpha(\mathbf{r}) \quad (26)$$

plays a key role in the development of the necessary conditions for problem RS. Note that this integral is a functional; hence, we call it the Riemann–Stieltjes I functional as a means to distinguish it from the cost or J functional.

In the same spirit, let $\nu \in \mathbb{R}_+^{N_c}$ be the nonnegative endpoint multiplier (covector) that satisfies the complementary slackness condition

$$\nu^T \left(\int_{\text{supp}(\mathbf{r})} \mathbf{e}(\mathbf{r}) d\alpha(\mathbf{r}) \right) = \int_{\text{supp}(\mathbf{r})} \nu^T \mathbf{e}(\mathbf{r}) d\alpha(\mathbf{r}) = 0$$

Then, the endpoint Lagrangian [6] is defined as

$$\tilde{E}(\nu, \mathbf{r}) := E(\mathbf{r}) + \nu^T \mathbf{e}(\mathbf{r}) \quad (27)$$

To derive the necessary conditions, we begin by considering a sequence of Riemann–Stieltjes sum approximations to the cost functional and pass to the limit. For greater mathematical rigor, we should consider a Lebesgue–Stieltjes formulation; however, as noted in Sec. I, to limit the scope of this paper to engineering mathematics, we consider the simpler Riemann sums.

A. Riemann–Stieltjes Sum Approximation

Let $\delta \mathbf{r}_i, i = 1 \dots n$ be a collection of n nonoverlapping partitions of $\text{supp}(\mathbf{r})$ such that

$$\bigcup_{i=1}^n \delta \mathbf{r}_i = \text{supp}(\mathbf{r})$$

Let the sequence $\{n\}_{n \in \mathbb{N}}$ be such that

$$\max_i m(\delta \mathbf{r}_i) \rightarrow 0 \quad \text{as } n \rightarrow \infty$$

where $m(\delta \mathbf{r})$ is the N_r -dimensional volume

$$\prod_{j=1}^{N_r} \delta r_j$$

of $\delta \mathbf{r}$. Let $\mathbf{r}_i^*, i = 1, \dots, n$ be a corresponding collection of random variables having constant PDFs, over each $\delta \mathbf{r}_i$, and let Δ_α denote the discretization of the integrator α given by

$$\Delta_\alpha(\mathbf{r}^*, \delta \mathbf{r}) := \rho_c(\mathbf{r}^*) m(\delta \mathbf{r})$$

where $\rho_c(\mathbf{r}^*)$ is a constant over $\delta \mathbf{r}$. Then, under appropriate technical conditions [1,2,10], a Riemann–Stieltjes integral can be written as the limit of Riemann–Stieltjes sums

$$\int_{\text{supp}(\mathbf{r})} E(\mathbf{r}) d\alpha(\mathbf{r}) = \lim_{n \rightarrow \infty} \sum_{i=1}^n E(\mathbf{r}_i^*) \Delta_\alpha(\mathbf{r}_i^*, \delta \mathbf{r}_i) \quad (28)$$

Similarly, the endpoint integral constraint equation can be “discretized” as

$$\int_{\text{supp}(\mathbf{r})} \mathbf{e}(\mathbf{r}) d\alpha(\mathbf{r}) = \lim_{n \rightarrow \infty} \sum_{i=1}^n \mathbf{e}(\mathbf{r}_i^*) \Delta_\alpha(\mathbf{r}_i^*, \delta \mathbf{r}_i) \quad (29)$$

Hence, from Eqs. (27–29), we can write

$$\begin{aligned} \int_{\text{supp}(\mathbf{r})} \tilde{E}(\nu, \mathbf{r}) d\alpha(\mathbf{r}) &:= \int_{\text{supp}(\mathbf{r})} (E(\mathbf{r}) + \nu^T \mathbf{e}(\mathbf{r})) d\alpha(\mathbf{r}) \\ &= \lim_{n \rightarrow \infty} \sum_{i=1}^n (E(\mathbf{r}_i^*) + \tilde{\nu}_n^T \mathbf{e}(\mathbf{r}_i^*)) \Delta_{\alpha_i} \end{aligned} \quad (30)$$

where we have used the shorthand notation $\Delta_{\alpha_i} := \Delta_\alpha(\mathbf{r}_i^*, \delta \mathbf{r}_i)$ and assumed a sequence $\{\tilde{\nu}_n\} \rightarrow \nu$ as $n \rightarrow \infty$.

Motivated by these formulas, we define a semidiscretization of Eq. (10) over $\text{supp}(\mathbf{r})$ as

$$\begin{aligned} \dot{\mathbf{x}}_1 &= \mathbf{f}(\mathbf{x}_1, \mathbf{u}) \\ \dot{\mathbf{x}}_2 &= \mathbf{f}(\mathbf{x}_2, \mathbf{u}) \\ &\vdots \\ \dot{\mathbf{x}}_n &= \mathbf{f}(\mathbf{x}_n, \mathbf{u}) \end{aligned} \quad (31)$$

where $\dot{\mathbf{x}}_i$ is a shorthand notation for the time derivative of $\mathbf{x}(t, \mathbf{r}_i^*)$. The collection of systems represented by Eq. (31) is a system of n dynamic systems where the i th system is valid over a vanishingly small region $\delta \mathbf{r}_i$ over $\text{supp}(\mathbf{r})$. By analogy, it follows that a semidiscretization of Eq. (25) generates the collection of n adjoint dynamic systems

$$\begin{aligned} -\dot{\lambda}_1 &= \partial_x H(\lambda_1, \mathbf{x}_1, \mathbf{u}) \\ -\dot{\lambda}_2 &= \partial_x H(\lambda_2, \mathbf{x}_2, \mathbf{u}) \\ &\vdots \\ -\dot{\lambda}_n &= \partial_x H(\lambda_n, \mathbf{x}_n, \mathbf{u}) \end{aligned} \quad (32)$$

Hence, we can write Eq. (26) as

$$I[\lambda(t, \cdot), \mathbf{x}(t, \cdot), \mathbf{u}] = \lim_{n \rightarrow \infty} \sum_{i=1}^n \lambda_i^T(t) \mathbf{f}(\mathbf{x}_i(t), \mathbf{u}) \Delta_{\alpha_i} \quad (33)$$

Thus, for any fixed value of n , we can now construct a standard optimal control problem given by

$$\begin{aligned} \mathbf{x}_i &\in \mathbb{X} = \mathbb{R}^{N_x} \quad \forall i = 1, 2, \dots, n, \quad \mathbf{u} \in \mathbb{U} \subset \mathbb{R}^{N_u} \\ \text{(RS}^n \text{)} &\left\{ \begin{array}{l} \text{Minimize } J_n[\mathbf{x}_1(\cdot), \dots, \mathbf{x}_n(\cdot), \mathbf{u}(\cdot)] := \sum_{i=1}^n E(\mathbf{r}_i^*) \Delta_{\alpha_i} \\ \text{Subject to } \dot{\mathbf{x}}_1 = \mathbf{f}(\mathbf{x}_1, \mathbf{u}) \\ \vdots \\ \dot{\mathbf{x}}_n = \mathbf{f}(\mathbf{x}_n, \mathbf{u}) \\ \sum_{i=1}^n \mathbf{e}(\mathbf{r}_i^*) \Delta_{\alpha_i} \leq 0 \end{array} \right. \end{aligned} \quad (34)$$

B. Riemann–Stieltjes Generalization of Pontryagin’s Principle

Problem RS^n is a standard optimal control problem; hence, we can apply Pontryagin’s principle and construct the Hamiltonian function as

$$\begin{aligned} H_n(\tilde{\lambda}_1, \dots, \tilde{\lambda}_n, \mathbf{x}_1, \dots, \mathbf{x}_n, \mathbf{u}) &:= \tilde{\lambda}_1^T \mathbf{f}(\mathbf{x}_1, \mathbf{u}) + \dots + \tilde{\lambda}_n^T \mathbf{f}(\mathbf{x}_n, \mathbf{u}) \\ &= \sum_{i=1}^n \tilde{\lambda}_i^T \mathbf{f}(\mathbf{x}_i, \mathbf{u}) \end{aligned} \quad (35)$$

where $\tilde{\lambda}_i, i = 1, \dots, n$ are the adjoint covectors for problem RS^n that satisfy the adjoint differential equations

$$\begin{aligned} -\dot{\tilde{\lambda}}_1 &= \partial_{x_1} H_n(\tilde{\lambda}_1, \dots, \tilde{\lambda}_n, \mathbf{x}_1, \dots, \mathbf{x}_n, \mathbf{u}) \\ &\vdots \\ -\dot{\tilde{\lambda}}_n &= \partial_{x_n} H_n(\tilde{\lambda}_1, \dots, \tilde{\lambda}_n, \mathbf{x}_1, \dots, \mathbf{x}_n, \mathbf{u}) \end{aligned} \quad (36)$$

Comparing Eq. (33) with Eq. (35), we can write

$$\begin{aligned} \lim_{n \rightarrow \infty} H_n(\lambda_1(t) \Delta_{\alpha_1}, \dots, \lambda_n(t) \Delta_{\alpha_n}, \mathbf{x}_1(t), \dots, \mathbf{x}_n(t), \mathbf{u}) \\ = \lim_{n \rightarrow \infty} \sum_{i=1}^n \lambda(t) \mathbf{f}(\mathbf{x}_i(t), \mathbf{u}) \Delta_{\alpha_i} \\ = I[\lambda(t, \cdot), \mathbf{x}(t, \cdot), \mathbf{u}] \end{aligned} \quad (37)$$

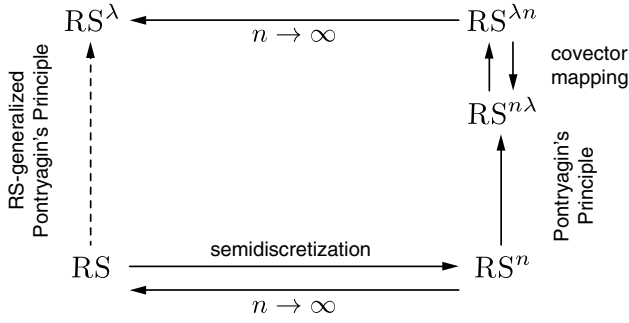


Fig. 4 Schematic of the derivation of a Riemann–Stieltjes-generalized Pontryagin principle facilitated through a new application of the covector mapping principle.

This suggests that the adjoints of problem RS^n transform to the semidiscrete adjoints of problem RS according to

$$\frac{\tilde{\lambda}_i(t)}{\Delta_{ai}} = \lambda_i(t) \quad i = 1, \dots, n \quad (38)$$

It can be verified by direct substitution that this transformation is consistent with Eq. (32) and Eq. (36) as well.

Applying the Hamiltonian minimization condition [6] to Problem RS^2 , we get

$$\begin{aligned} \mathbf{u}_n^*(t) &= \arg \min_{u(t) \in \mathbb{U}} \sum_{i=1}^n \tilde{\lambda}_i^T \mathbf{f}(\mathbf{x}_i, \mathbf{u}(t)) \\ &= \arg \min_{u(t) \in \mathbb{U}} \sum_{i=1}^n \lambda_i^T \mathbf{f}(\mathbf{x}_i, \mathbf{u}(t)) \Delta_{ai} \end{aligned} \quad (39)$$

where the last equality in Eq. (39) follows from Eq. (38). Passing to the limit $n \rightarrow \infty$, we arrive at

$$\begin{aligned} \mathbf{u}^*(t) &= \arg \min_{u(t) \in \mathbb{U}} I[\lambda(t, \cdot), \mathbf{x}(t, \cdot), \mathbf{u}(t)] \\ &= \arg \min_{u(t) \in \mathbb{U}} \int_{\text{supp}(r)} H(\lambda(t, \mathbf{r}), \mathbf{x}(t, \mathbf{r}), \mathbf{u}(t)) d\alpha(\mathbf{r}) \end{aligned} \quad (40)$$

The transversality condition can be derived similarly. The endpoint Lagrangian for problem RS^n is given by

$$\sum_{i=1}^n E(\mathbf{r}_i^*) \Delta_{ai} + \nu_n^T \sum_{i=1}^n \mathbf{e}(\mathbf{r}_i^*) \Delta_{ai}$$

Hence, an application of the transversality conditions generates

$$\begin{aligned} (-\tilde{\lambda}(t_0, \mathbf{r}_j^*), \tilde{\lambda}(t_f, \mathbf{r}_j^*)) &= \frac{\partial}{\partial \mathbf{r}_j^*} \left(\sum_{i=1}^n (E(\mathbf{r}_i^*) + \nu_n^T \mathbf{e}(\mathbf{r}_i^*)) \Delta_{ai} \right) \\ &= \sum_{i=1}^n \frac{\partial}{\partial \mathbf{r}_j^*} ((E(\mathbf{r}_i^*) + \nu_n^T \mathbf{e}(\mathbf{r}_i^*)) \Delta_{ai}) \\ &= \left(\frac{\partial E(\mathbf{r}_j^*)}{\partial \mathbf{r}_j^*} + \left[\frac{\partial \mathbf{e}(\mathbf{r}_j^*)}{\partial \mathbf{r}_j^*} \right]^T \nu_n \right) \Delta_{aj} \quad j = 1, \dots, n \end{aligned} \quad (41)$$

Passing to the limit $n \rightarrow \infty$ and using Eq. (38), we get

$$(-\lambda(t_0, \mathbf{r}), \lambda(t_f, \mathbf{r})) = \frac{\partial \tilde{E}(\nu, \mathbf{r})}{\partial \mathbf{r}} \quad \forall \mathbf{r} \in \text{supp}(\mathbf{r}) \quad (42)$$

Thus, we have derived a Riemann–Stieltjes-generalized Pontryagin principle via a new application of the covector mapping principle [11–14] summarized in Fig. 4. Our results are similar to those obtained in [15,16] with key points of departure being in our models for the cost function and endpoint conditions.

C. Riemann–Stieltjes Versus Standard Optimal Control Problems

A consequential conclusion of Eq. (40) is that the Riemann–Stieltjes optimal control $t \mapsto \mathbf{u}_{RS}^*(t) \in \mathbb{U}$ is obtained by “optimizing the average” Pontryagin Hamiltonian and not by “averaging the optimized” controls. This follows from the fact that the arg min operation cannot be taken inside the integral; that is,

$$\begin{aligned} \arg \min_{u(t) \in \mathbb{U}} \int_{\text{supp}(r)} H(\lambda(t, \mathbf{r}), \mathbf{x}(t, \mathbf{r}), \mathbf{u}(t)) d\alpha(\mathbf{r}) \\ \neq \int_{\text{supp}(r)} \arg \min_{u(t) \in \mathbb{U}} H(\lambda(t, \mathbf{r}), \mathbf{x}(t, \mathbf{r}), \mathbf{u}(t)) d\alpha(\mathbf{r}) \end{aligned} \quad (43)$$

Because the operations arg min and \int are not commutative, generating an analytical solution to even a simple Riemann–Stieltjes optimal control problem is exceedingly difficult [11]. In fact, from Eq. (40) the optimal Riemann–Stieltjes control is determined for each t by a functional map

$$\mathbf{u}_{RS}: L^1 \times L^1 \rightarrow \mathbb{R}^{N_u}$$

which is in sharp contrast to standard optimal control that is given by an algebraic map $\mathbf{u}_{std}: \mathbb{R}^{N_x} \times \mathbb{R}^{N_x} \rightarrow \mathbb{R}^{N_u}$. In other words, while generating an expression for a Pontryagin optimal control requires a solution to a mathematical programming problem [6], the comparable problem for a Riemann–Stieltjes optimal control is a solution to the integrated Hamiltonian minimization (IHM) problem

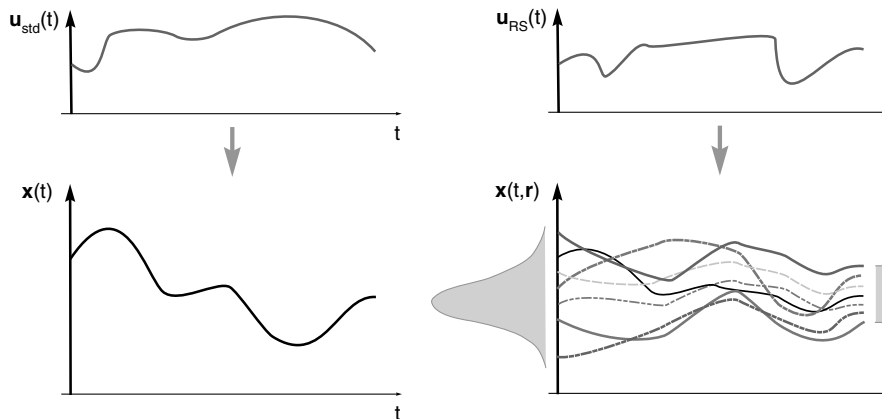


Fig. 5 Illustrating a key difference between a standard optimal control solution and a Riemann–Stieltjes optimal solution.

(IHM)

$$\times \begin{cases} \text{Minimize } I[\lambda(t, \cdot), \mathbf{x}(t, \cdot), \mathbf{u}] := \int_{\text{supp}(\mathbf{r})} H(\lambda(t, \mathbf{r}), \mathbf{x}(t, \mathbf{r}), \mathbf{u}) d\alpha(\mathbf{r}) \\ \text{Subject to } \mathbf{u} \in \mathbf{U} \end{cases}$$

which is a constrained functional optimization problem. Deferring for the moment a discussion of a computationally efficient method for solving such problems, note that a standard optimal control trajectory $t \mapsto \mathbf{u}_{\text{std}}^*(t)$ controls a single trajectory $t \mapsto \mathbf{x}^*(t)$ whereas a Riemann–Stieltjes optimal control $t \mapsto \mathbf{u}_{\text{RS}}^*(t)$ controls an entire trajectory tube $\{t \mapsto \mathbf{x}^*(t, \mathbf{r}) : \mathbf{r} \in \text{supp}(\mathbf{r})\}$. These points are illustrated in Fig. 5 where the Riemann–Stieltjes controlled trajectory tube starts out as a Gaussian distribution and is controlled by a single controller to a uniformly distributed collection over a compact support.

V. Computational Methods

Given that constructing a closed-form solution to a deterministic optimal control problem involves the extremely difficult problem of solving nonlinear differential-algebraic equations, it is not surprising that finding analytical solutions to a Riemann–Stieltjes optimal control problem is almost next to impossible. Even a computational method can be quite daunting because it involves devising an efficient numerical method to evaluate the multidimensional Riemann–Stieltjes integral. The simplest numerical method is a Monte Carlo technique; however, the value of n required for this approximation is typically extremely large ($> 10^4$). Drawing the connections between the fact that quadrature schemes are efficient numerical techniques for integral evaluation and that pseudospectral (PS) techniques [12,17–19] are based on quadrature points, we construct hyperpseudospectral (HS) methods that extend standard PS methods to solving the Riemann–Stieltjes optimal control problem. To facilitate this development, we first summarize a standard PS method and then extend it to higher-dimensional spaces.

A. Standard Pseudospectral Optimal Control Theory

As surveyed in Ross and Karpenko [12], standard PS optimal control theory is founded on expressing the state trajectory $\mathbf{x}(\cdot)$ as an infinite series expansion

$$\mathbf{x}(t) = \sum_{m=0}^{\infty} \mathbf{a}_m P_m(t) \quad (44)$$

where $P_m(t)$ is a polynomial in t of degree m . If $P_m(t)$ is chosen to be a Legendre polynomial of degree m , the infinite series gives rise to a Legendre PS method. Similarly, if $P_m(t)$ are chosen to be Chebyshev polynomials, we generate a Chebyshev PS method. Typical choices in PS optimal control theory are these “big two” methods [12] because other polynomial basis functions do not have desirable properties for optimal control applications [19,20].

The coefficients \mathbf{a}_m in Eq. (44) are called the spectral coefficients [17,18,21]. A key principle in a PS approach is that the spectral coefficients are computed indirectly by transforming Eq. (44) to the space of Lagrange interpolating polynomials. Thus, Eq. (44) may be written equivalently as [12,22,23]

$$\mathbf{x}(t) = \sum_{j=0}^{\infty} \mathbf{b}_j \frac{W(t)}{W(t_j)} \phi_j(t) \quad (45)$$

where t_j , $j = 0, 1, 2, \dots$ are discrete points in time called nodes, $W(t)$ is a weight function, and $\phi_j(t)$ is a Lagrange interpolating polynomial that satisfies the Kronecker relationship

$$\phi_j(t_k) = \delta_{jk} \quad (46)$$

Satisfaction of the Kronecker relationship implies that

$$\mathbf{x}(t_k) = \sum_{j=0}^{\infty} \mathbf{b}_j \frac{W(t_k)}{W(t_j)} \phi_j(t_k) = \mathbf{b}_k \quad (47)$$

That is, the coefficient \mathbf{b}_j in Eq. (45) is the value of $\mathbf{x}(t)$ at $t = t_j$. It is this “sampling” property, which is absent in Eq. (44), that makes a PS approach distinct from the direct use of Eq. (44).

In practice, Eq. (45) cannot be implemented due to infinite summation [the same is true of Eq. (44)]. The best one can expect to achieve is a solution up to machine precision $\epsilon_m > 0$. In a series of theorems developed by Gong, Kang, Fahroo, and Ross (summarized in [12,14,24–27]), it was proved that if $\mathbf{x}^*(\cdot)$ is the optimal solution, then, given any $\epsilon > 0$, there exists an $N = N_\epsilon$ such that $\|\mathbf{x}^{N_\epsilon}(\cdot) - \mathbf{x}^*(\cdot)\| \leq \epsilon$ with $\mathbf{x}^{N_\epsilon}(t)$ given by

$$\mathbf{x}^{N_\epsilon}(t) = \sum_{j=0}^{N_\epsilon} \frac{W(t)}{W(t_j)} \phi_j(t) \mathbf{x}_j \quad (48)$$

where we have replaced the notation \mathbf{b}_j by \mathbf{x}_j , a more evocative notation that recognizes the sampling property given by Eq. (47). Although the practice of PS techniques requires that $\epsilon \geq \epsilon_m$, the theory allows ϵ to go to zero in the limit

$$\lim_{N_\epsilon \rightarrow \infty} \mathbf{x}^{N_\epsilon}(t) = \mathbf{x}^*(t) \quad \text{for almost all } t \in [t_0, t_f] \quad (49)$$

This is why PS optimal control theory is called a joint theoretical-computational approach to solving (standard) optimal control problems.

It can be shown that the best PS points t_j , $j = 0, 1, 2, \dots$ are indeed quadrature points [17,18]. Hence, we now aim to seek the best cubature points to discretize the Riemann–Stieltjes J functional.

B. Hyper-Pseudospectral Concepts

Hyper-pseudospectral theory extends pseudospectral theory from the one-dimensional t domain to the multidimensional $t \times \mathbf{r}$ domain. If $N_r = 1$, we can approximate the Riemann–Stieltjes J functional using standard quadrature points. When $N_r \geq 2$, Kronecker products of one-dimensional quadrature points are not the minimal set of points for generating efficient cubature formulas [28,29]. This implies that we can generate fewer than $(N_{\text{PS}})^{N_r}$ points for cubature when $N_r \geq 2$ where N_{PS} are the number of PS points in one dimension. Based on this existence result, we seek to produce an efficient cubature formula for

$$\mathcal{J}[E] := \int_{\text{supp}(\mathbf{r})} E(\mathbf{r}) d\alpha(\mathbf{r}) \quad (50)$$

so that problem RS^n can be posed with the smallest possible number n . When α is differentiable, we can write Eq. (50) in its Riemann form

$$\mathcal{J}[E] := \int_{\text{supp}(\mathbf{r})} E(\mathbf{r}) \rho(\mathbf{r}) d\mathbf{r} \quad (51)$$

which indicates that the PDF serves as the weight function for generating cubature formulas. Hence, we can get cubature points that are optimized for a given PDF. A cubature formula for Eq. (50) is of the form

$$\mathcal{J}[E] := \sum_{j=1}^n w_j E(\mathbf{r}_j) + \text{Res}[E] \quad (52)$$

where $\text{Res}[E]$ is the error; w_j are called weights and \mathbf{r}_j are called nodes. From Eq. (50), we have $\mathcal{J}[1] = 1$; hence, we choose weights that satisfy the condition

$$\sum_{j=1}^n w_j = 1, \quad \text{Res}[1] = 0 \quad (53)$$

We generate the summation in Eq. (52) through multidimensional polynomials as follows: Let $\mathbf{m} := (m_1, m_2, \dots, m_{N_r}) \in \mathbb{N}^{N_r}$ be an N_r -dimensional vector of integers; then

$$\mathbf{r}^{\mathbf{m}} := r_1^{m_1} r_2^{m_2} \dots r_{N_r}^{m_{N_r}}$$

is called a monomial of degree

$$|\mathbf{m}| := \sum_{i=1}^{N_r} m_i$$

(of N_r variables). A polynomial $P_m(\mathbf{r}) = P_m(r_1, r_2, \dots, r_{N_r})$ of degree $|\mathbf{m}|$ can be represented as

$$P_m(\mathbf{r}) = \sum_{s=0}^m \sum_{|\mathbf{k}|=s} a_{\mathbf{k}} \mathbf{r}^{\mathbf{k}}$$

where

$$\sum_{|\mathbf{k}|=s}$$

implies summation over all multi-indices of length s . If the moments

$$\mathcal{J}[\mathbf{r}^{\mathbf{m}}] = \int_{\text{supp}(r)} \mathbf{r}^{\mathbf{m}} d\alpha(\mathbf{r}) \quad \mathbf{m} \in \mathbb{N}^{N_r}$$

exist, then the monomial basis can be orthogonalized by the Gram–Schmidt process [28]. Let $\mathcal{J}_n[E]$ denote the cubature of $\mathcal{J}[E]$; that is, let

$$\mathcal{J}_n[E] := \sum_{j=1}^n w_j E(\mathbf{r}_j) \quad (54)$$

then the monomial basis can be set up, in principle, by moment cubatures

$$\mathcal{J}[\mathbf{r}^{\mathbf{m}}] = \mathcal{J}_n[\mathbf{r}^{\mathbf{m}}] \Rightarrow \int_{\text{supp}(r)} \mathbf{r}^{\mathbf{m}} d\alpha(\mathbf{r}) = \sum_{j=1}^n w_j \mathbf{r}_j^{\mathbf{m}}$$

The moments $\mathcal{J}[\mathbf{r}^{\mathbf{m}}]$ can be computed using moment-generating functions for any given α : $\text{supp}(\mathbf{r}) \mapsto \mathbb{R}$. For the determination of HS points, we allow the cubature conditions to be satisfied approximately and stipulate that the moments be inside of some region

$$L_m \leq \mathcal{J}[\mathbf{r}^{\mathbf{m}}] - \sum_{j=1}^n w_j \mathbf{r}_j^{\mathbf{m}} \leq U_m \quad (55)$$

where L_m and U_m are the lower and upper bounds of the region that define an $\varepsilon > 0$ box. In addition, the HS points are required to lie inside of $\text{supp}(\mathbf{r})$ while minimizing some appropriate measure of error $\text{Res}[E]$, leading to the mixed integer nonlinear multi-objective programming problem

$$\begin{aligned} n \in \mathbb{N}, \quad (w_1, \dots, w_n) \in \mathbb{R}_+^n, \quad (\mathbf{r}_1, \dots, \mathbf{r}_n) \in \text{supp}(\mathbf{r}) \times \mathbb{R}^n \\ \left\{ \begin{array}{l} \text{Minimize} \quad (\text{Res}[\mathbf{r}^{\mathbf{m}}], n) \\ \text{Subject to} \quad L_1 \leq \mathcal{J}[\mathbf{r}^{\mathbf{1}}] - \sum_{j=1}^n w_j \mathbf{r}_j^{\mathbf{1}} \leq U_1 \\ \quad \quad \quad \vdots \\ \quad \quad \quad L_m \leq \mathcal{J}[\mathbf{r}^{\mathbf{m}}] - \sum_{j=1}^n w_j \mathbf{r}_j^{\mathbf{m}} \leq U_m \\ \quad \quad \quad \sum_{j=1}^n w_j = 1 \end{array} \right. \quad (56) \end{aligned}$$

For a fixed n , problem HS_m is a nonlinear programming problem. Thus, this problem is quite tractable and the HS points can be

generated for various values of the degree $|\mathbf{m}|$. Because the value of n generated by this approach is far less than the number of random points needed to produce comparable accuracy [30], we distinguish our technique from the standard Monte Carlo as the Monte Rey simulation. Under appropriate conditions on problem HS_m , the HS points reduce to the Hermite–Gauss nodes and the sigma points introduced by Julier et al. [31,32] to design nonlinear filters. Hence, an unscented optimal control problem [8,9] is simply a particular semidiscretization of the Riemann–Stieltjes optimal control problem.

VI. Ground Test Results on the Honeywell Testbed

Many space applications involve solving a multipoint optimal control problem [33]. The sequence of optimal control problems is dictated by mission requirements and many other practical constraints. In a typical attitude slew problem [34–37], a spacecraft is required to point and repoint to various orientations that can be framed in terms of arbitrary boundary conditions on the quaternion $\mathbf{q} \in \mathbb{R}^4$ and angular velocity $\boldsymbol{\omega} \in \mathbb{R}^3$. The attitude dynamics of a spacecraft driven by a collection of single-gimbal control moment gyroscopes (CMGs) is given by [38]

$$\begin{aligned} \begin{bmatrix} \dot{\mathbf{q}} \\ \dot{\boldsymbol{\omega}} \\ \dot{\boldsymbol{\delta}} \end{bmatrix} &:= \dot{\mathbf{x}} = \mathbf{f}(\mathbf{x}, \mathbf{u}) \\ &:= \begin{bmatrix} \frac{1}{2} \mathbf{Q}(\boldsymbol{\omega}) \mathbf{q} \\ \mathbf{I}^{-1}(-\boldsymbol{\omega} \times \mathbf{I} \cdot \boldsymbol{\omega} - \boldsymbol{\omega} \times \mathbf{h}(\boldsymbol{\delta}) - \mathbf{A}(\boldsymbol{\delta}) \mathbf{u}) \\ \mathbf{u} \end{bmatrix} \end{aligned} \quad (57)$$

where $\boldsymbol{\delta} \in \mathbb{R}^{N_{\text{cmgs}}}$ is the vector of gimbal angles, N_{cmgs} is the number of CMGs, and $\mathbf{h}(\boldsymbol{\delta})$ is the angular momentum of the CMG configuration. A CMG configuration is said to be in a singular state if the $3 \times N_{\text{cmgs}}$ matrix $\mathbf{A}(\boldsymbol{\delta})$ is singular. In addition to time optimality, a key requirement for CMG maneuverability is singularity avoidance; that is, it is highly desirable to design trajectories that are far away from the regions where $\mathbf{A}(\boldsymbol{\delta})$ is singular. A practical measure of the singularity condition is given by [39]

$$S(\boldsymbol{\delta}) := \sqrt{\det[\mathbf{A}(\boldsymbol{\delta}) \mathbf{A}^T(\boldsymbol{\delta})]}$$

When $S(\boldsymbol{\delta})$ is zero, the spacecraft is essentially uncontrollable; hence, we can frame an optimality criterion for maneuverability as the maximization of the Chebyshev cost functional

$$\min_{t \in [t_0, t_f]} S(\boldsymbol{\delta}(t))$$

Thus, a spacecraft maneuvering problem may be posed as a multi-objective optimal control problem [6], with a two-dimensional vector cost functional \mathbf{J} given by

$$\mathbf{J}[\mathbf{x}(\cdot), \mathbf{u}(\cdot), t_f] := \begin{bmatrix} t_f \\ -\min_{t \in [t_0, t_f]} S(\boldsymbol{\delta}(t)) \end{bmatrix} \quad (58)$$

The constraints on this cost functional are the dynamics of Eq. (57) and arbitrary but given boundary conditions [36,37].

A. Ground Test Setup and Initial Results

The U.S. Air Force Research Laboratory's miniature momentum control system (MMCS) is a set of $N_{\text{cmgs}} = 4$ CMGs arranged in a box configuration to provide three-axis control of a spacecraft. The \mathbf{A} matrix for this configuration is given by

$$\mathbf{A}(\boldsymbol{\delta}) = \begin{bmatrix} 0 & \sin(\delta_2) & 0 & -\sin(\delta_4) \\ \cos(\delta_1) & \cos(\delta_2) & \cos(\delta_3) & \cos(\delta_4) \\ \sin(\delta_1) & 0 & -\sin(\delta_3) & 0 \end{bmatrix} \quad (59)$$

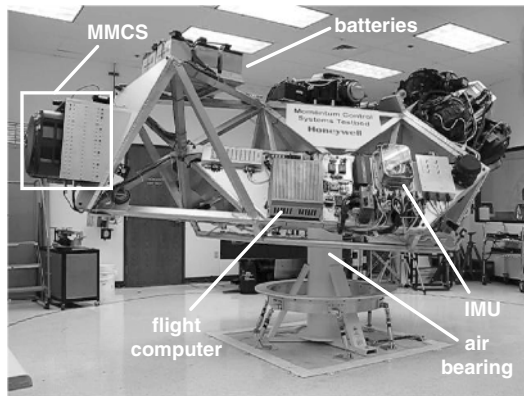


Fig. 6 Honeywell's 3000 lb MCS ground testbed outfitted with the U.S. Air Force Research Laboratory's MMCS. (IMU, inertial measurement unit.)

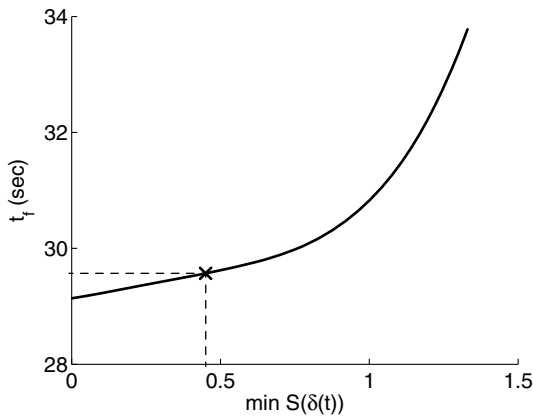


Fig. 7 Pareto front and decision point for the multi-objective cost functional given by Eq. (58).

During the summer of 2013, the MMCS was set up for ground testing at Honeywell as part of a guest investigator program. The Honeywell momentum control system (MCS) testbed outfitted with the MMCS is shown in Fig. 6. This system is about 3000 lb and floats on an air bearing at Honeywell's test facility near Phoenix, Arizona. Because the MMCS is mounted off center, the system is balanced to align the testbed center of gravity with the center of rotation. After coarse manual balancing, automatic balancing is performed via a set of three prismatic actuators with fine position control to locate a series of masses to drive the center of mass to the air bearing pivot.

The Pareto front of \mathbf{J} for this setup is shown in Fig. 7. Each point on the Pareto front was computed using DIDO, a MATLAB application package[†] for solving optimal control problems [40]. Using the decision-maker (DM) concept, we chose the Pareto-optimal point

$$\mathbf{J}_{\text{DM}}[\mathbf{x}^1(\cdot), \mathbf{u}^1(\cdot), t_f^1] := \begin{bmatrix} 29.6 \\ -0.45 \end{bmatrix} \quad (60)$$

for ground test implementation. The Pareto-optimal control for this decision and a representative motion of the MCS in a projected quaternion space is shown in Fig. 8. An experimental implementation of the result, shown in Fig. 9, reveals that the MCS failed this test. Upon postexperimental analysis, we concluded that the reason for this failure is due to the singularity index going to zero in the actual experiment. That is, despite the fact that we chose

$$\max \min_{t \in [t_0, t_f]} S(\delta(t)) = 0.45$$

the actual value of this cost in the experiment was zero. This discovery is shown in Fig. 10, which shows a plot of $t \mapsto S(\delta)$ from which it is apparent that the MCS goes into a singular state at $t \approx 20$ s. Additional experiments were performed to validate this analysis.

B. Riemann–Stieltjes Solution and Its Implementation

Although Fig. 10 explains the reason for the failure, it does not explain its cause. Upon further analysis of the results, we concluded that the cause of the failure was due to “gimbal drift” and accumulation of angular momentum caused by various disturbances in the setup. Not only are these disturbances practical, they are also representative of flight conditions. The effect of these disturbances manifests itself in the form of imprecise knowledge in $\delta(t_0)$. This analysis suggests that we can formulate a Riemann–Stieltjes cost functional as

$$J_{\text{RS}}[\mathbf{x}(\cdot, \cdot), \mathbf{u}(\cdot), t_f] := \int_{\text{supp}(\delta^0)} J_{\text{unc}}[\mathbf{x}(\cdot, \delta^0), \mathbf{u}(\cdot)] d\alpha(\delta^0) \quad (61)$$

where the map $\delta^0 \mapsto J_{\text{unc}}$ is given by

$$J_{\text{unc}}[\mathbf{x}(\cdot, \delta^0), \mathbf{u}(\cdot)] := - \min_{t \in [t_0, t_f]} S(\delta(t); \delta^0) \quad (62)$$

We assumed the CDF $\alpha: \mathbb{R}^4 \ni \delta^0 \mapsto \mathbb{R}$ to be uncorrelated Gaussian with $\sigma = 10$ deg standard deviation in each gimbal angle. The Riemann–Stieltjes optimal control for these set of assumptions is shown in Fig. 11. The optimal control was computed by using DIDO and incorporating many of the results presented in this paper. Also shown in Fig. 11 is the state trajectory tube (cf. Fig. 5) in the projected quaternion space. That the Riemann–Stieltjes control does indeed control a state trajectory tube is more apparent in the inset of Fig. 11, which shows a collection of trajectories being controlled to the desired target point. Comparing this figure with Fig. 8, it is clear that the Riemann–Stieltjes optimal control is quite different from the standard optimal control. An experimental implementation of the result, shown in Fig. 12, indicates a complete success of this test. As a means to ratify our previous analysis on the cause of the failure of the standard optimal control, we show in Fig. 13 a plot of the singularity index function $t \mapsto S(\delta)$ for the test run of Fig. 12. Clearly, in contrast to Fig. 10, this time we have

$$\min_{t \in [t_0, t_f]} S(\delta(t)) \neq 0$$

In fact, the experimental value of the Chebyshev cost can be read off the graph; this value is 0.86.

Although a single experiment is sufficient to show failure, multiple, repeatable, successful experiments are necessary to demonstrate operational viability. In view of this requirement for operational transition, we conducted several additional tests at Honeywell. These additional tests are, by nature, random in the sense that we do not know in advance the value of the initial gimbal angle $\delta(t_0)$. The results of these trials are shown in Fig. 14. The inset in Fig. 14 clearly shows successful completion of the maneuvers achieved via the same, unmodified Riemann–Stieltjes control, under the absence of knowledge of the initial gimbal angles. The gimbal angle trajectory tubes for each of these trials is shown in Fig. 15.

VII. Further Applications and Open Problems in Riemann–Stieltjes Optimal Control Theory

Starting with Eq. (1), it has been evident that our model of an uncertain dynamic system is different from the Itô differential equation [41,42]

$$d\mathbf{x} = \mathbf{f}(\mathbf{x}, \mathbf{u}, t) dt + \sigma(\mathbf{x}, \mathbf{u}, t) d\mathbf{W} \quad (63)$$

where \mathbf{W} is the standard Wiener process and σ is a given matrix-valued diffusion function. Because of the fundamental difference between Eqs. (1) and (63), Riemann–Stieltjes optimal control

[†]Data available online at http://www.mathworks.com/products/connections/product_detail/product_61633.html [retrieved 7 July 2014].

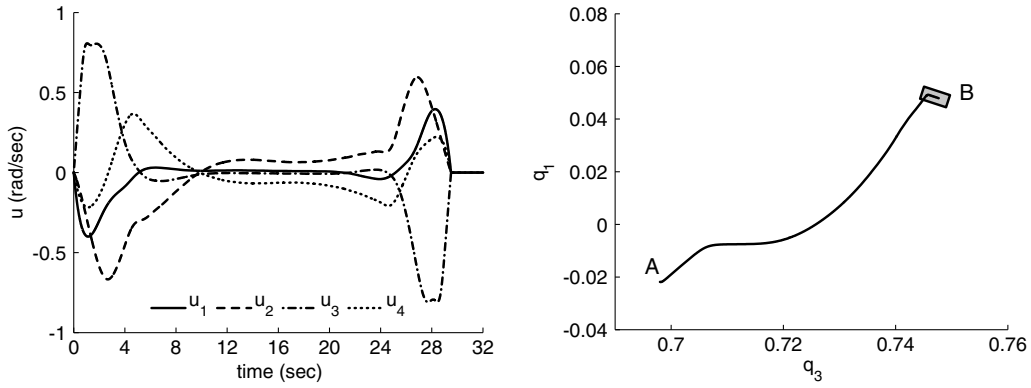


Fig. 8 Pareto-optimal control trajectory and representative simulated motion of the MCS in a projected quaternion space.

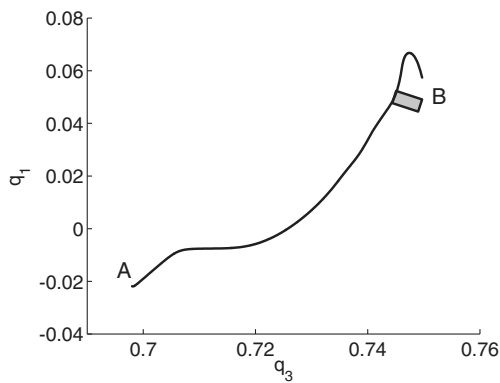


Fig. 9 Experimental result of the motion of the MCS in the same projected quaternion space as Fig. 8.

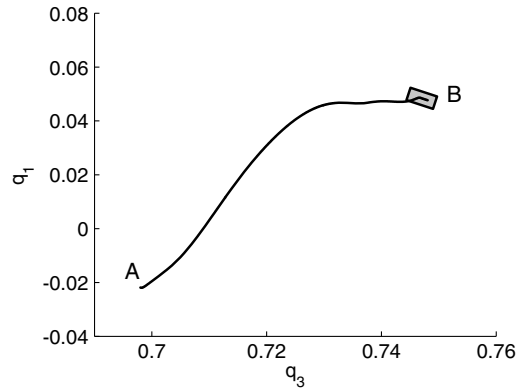


Fig. 12 Ground test result of an implementation of the Riemann–Stieltjes control illustrating the motion of the MCS in the same projected quaternion space as Fig. 8.

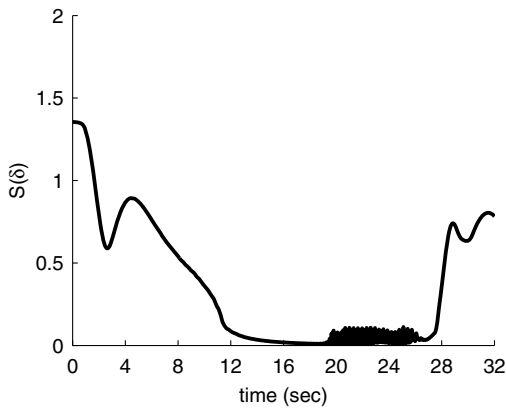


Fig. 10 Experimental results for the “running cost” of the Chebyshev cost functional.

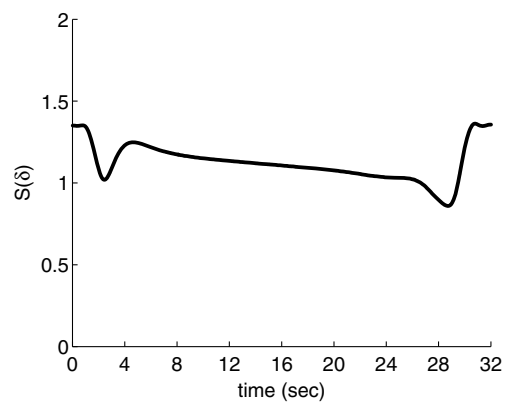


Fig. 13 Experimental result of the singularity index function for the maneuver shown in Fig. 12.

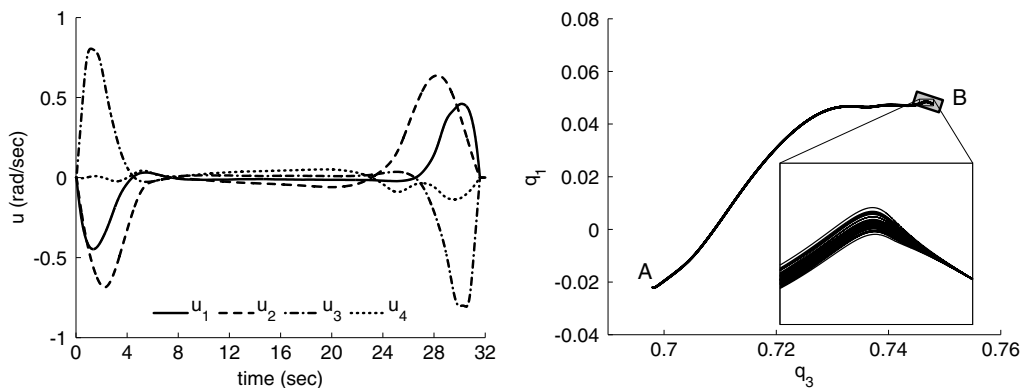


Fig. 11 Riemann–Stieltjes optimal control trajectory and a simulated state trajectory tube of the MCS in the same projected quaternion space as Fig. 8.

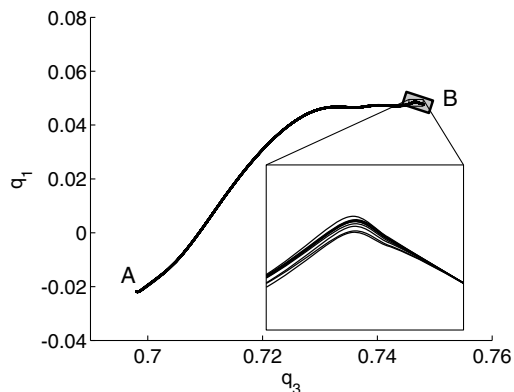


Fig. 14 Repeatable ground test results of the motion of the MCS for random trials.

problems are entirely different from previous stochastic optimal control problems [43]. As a means to distinguish the difference between these two choices of modeling uncertain dynamic systems, we follow Aubin et al. [44] and call Eq. (1) a controlled tychastic differential equation, where \mathbf{p} is a “tychastic” parameter. We would have called \mathbf{p} a “random” parameter if, according to Aubin et al. [44,45], the “terminology [was not] already confiscated by probability theory.” Tyches means “chance” in classical Greek, from the Goddess Tyche [44]. By borrowing the connection between a controlled differential equation and a differential inclusion [46], we can transform Eq. (1) to a controlled differential inclusion

$$\dot{\mathbf{x}} \in \mathcal{F}(\mathbf{x}, \mathbf{u}, t) := \{\mathbf{f}(\mathbf{x}, \mathbf{u}, t; \mathbf{p}) : \mathbf{p} \in \text{supp}(\mathbf{p})\} \quad (64)$$

Thus, the evolution $t \mapsto \mathbf{x}$ is set valued but not random. In other words, we can regard $\dot{\mathbf{x}} = \mathbf{f}(\mathbf{x}, \mathbf{u}, t; \mathbf{p})$ as simply a parameterized model of a controlled evolutionary system that is subject to tychastic uncertainties [44]. In this context, the maxmin (“minimax”) Riemann–Stieltjes optimal control [see Eqs. (61) and (62)] that was implemented at Honeywell was a form of tychastic control (or “robust” control). Standard minimax optimal control problems are connected to the computation of viability kernels and capture basins [7,47,48], which form the central concepts in viability theory.

Viability theory was initiated in the late 1970s [7,49] to mathematically address the dynamics of socioeconomic, biological and other organizational systems that evolve in a Darwinian manner. The evolutionary engine is modeled as a differential inclusion $\dot{\mathbf{x}} \in \mathcal{F}(\mathbf{x})$. Given the large scope of viability theory, it is apparent that there are now an even larger number of open problems and opportunities to connect viability theory, particularly tychastic viability [50], with Riemann–Stieltjes optimal control theory. Thus, although our development of the Riemann–Stieltjes optimal control problem was motivated by a need to manage uncertainties in engineering systems, it is clear from the preceding discussion that problem RS can be used to connect concepts from viability theory. It turns out that many more independently developed ideas across disparate disciplines [8,51–58] can also be connected to a Riemann–Stieltjes optimal control problem. We briefly summarize these additional connections to illustrate some unification concepts and open problems while noting that the following discussions are no way meant to be exhaustive.

In search theory [51], the problem is to find a moving target (missing boat, lost hiker, fugitive, etc.) whose location $\mathbf{x}^T \in \mathbb{X}^T \subset \mathbb{R}^{N,T}$ is unknown. We assume the motion of the target $t \mapsto \mathbf{x}^T$ is conditionally deterministic: That is, the trajectory of the target conditioned on an uncertain vector \mathbf{p} is given by $\mathbf{x}^T(\cdot, \mathbf{p})$. A searcher (satellite, unmanned aerial vehicle, etc.) at \mathbf{x}^S is equipped with a sensor suite whose effectiveness is modeled [59] by an instantaneous probability density function called the search density function $\psi: (\mathbf{x}^T, \mathbf{x}^S) \mapsto \mathbb{R}_+$. The probability that the searcher will find the target by searching along a given trajectory $\mathbf{x}^S(\cdot)$ over a time interval $(0, t]$ is given by [51,59]

$$P(t, \mathbf{x}^T(t); \mathbf{p}) = 1 - \exp\left(-\int_0^t \psi(\mathbf{x}^S(\tau), \mathbf{x}^T(\tau, \mathbf{p})) d\tau\right)$$

Then, the probability that the searcher will detect the target over the time period $(0, t]$ is given by

$$\begin{aligned} & \int_{\text{supp}(p)} P(t, \mathbf{x}^T(t, \mathbf{p})) d\alpha(\mathbf{p}) \\ &= 1 - \int_{\text{supp}(p)} \exp\left(-\int_0^t \psi(\mathbf{x}^S(\tau), \mathbf{x}^T(\tau, \mathbf{p})) d\tau\right) d\alpha(\mathbf{p}) \end{aligned}$$

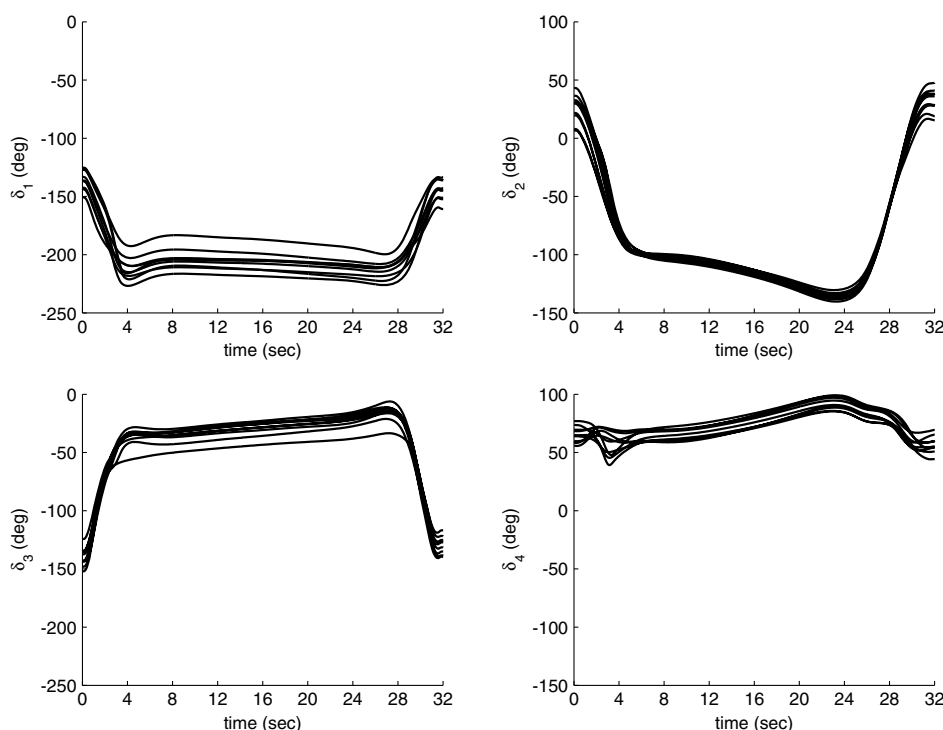


Fig. 15 Gimbal angle trajectory tubes for the ground test results corresponding to the random trials of Fig. 14.

where α is the CDF of \mathbf{p} . Thus, the quantity

$$\int_{\text{supp}(p)} \exp\left(-\int_0^t \psi(\mathbf{x}^S(\tau), \mathbf{x}^T(\tau, \mathbf{p})) d\tau\right) d\alpha(\mathbf{p})$$

represents the probability of nondetection. Let the searcher's dynamics be given by the deterministic dynamics $\dot{\mathbf{x}}^S = \mathbf{f}(\mathbf{x}^S, \mathbf{u})$. Then, we can define the optimal search problem as the problem of minimizing the Riemann–Stieltjes J functional

$$J(\mathbf{x}(\cdot, \cdot), \mathbf{u}(\cdot), t_f) \\ := \int_{\text{supp}(p)} \exp\left(-\int_0^{t_f} \psi(\mathbf{x}^S(t), \mathbf{x}^T(t, \mathbf{p})) dt\right) d\alpha(\mathbf{p})$$

where $\mathbf{x} := (\mathbf{x}^T, \mathbf{x}^S)$. Quadrature-based computational methods and the consistency of their approximations to solve this problem are analyzed in [60,61].

In quantum control, the objective is to design an electromagnetic input $t \mapsto \mathbf{u}$ to manipulate systems at the quantum level [62]. The applications of this concept are quite broad: from an ability to control molecules to produce new materials to medical imaging using nuclear magnetic resonance spectroscopy. Because the dynamics of the quantum “particles” are on the scale of Avogadro's number, it is far simpler to model the system as a continuum [63]; hence, in a quantum dynamic model $\dot{\mathbf{x}} = \mathbf{f}(\mathbf{x}, \mathbf{u}, t; p)$, the parameter p is a representation of this continuum. Li et al. [64] have pioneered a multidimensional PS method to optimally control this ensemble, by discretizing p over a Legendre–Gauss–Lobatto (LGL) grid. Thus, the LGL quantum particles p_i are controlled by electromagnetic pulses through a minimization of a discretized Riemann integral

$$\int_{\Omega} E(\mathbf{x}(t_f; p), t_f) dp \approx \sum_{i=0}^N E(\mathbf{x}(t_f; p_i), t_f) w_i$$

where $p_i \in \Omega \subset \mathbb{R}$ are the LGL points and w_i are the LGL weights. It is clear that the Riemann–Stieltjes optimal control problem generalizes the quantum optimal control problem.

Following similar reasoning, it is not too difficult to show that many other independently developed ideas [54–57] to solve specific problems in different applications can either be framed under, or tied in some manner to, the constructs of problem RS. There is no doubt that a vast body of research needs to be done in furthering these connections and advancing the applications and computational techniques. Great care must be exercised in formulating an application-specific Riemann–Stieltjes optimal control problem because of the increased severity of the issues related to the existence of a solution [8,9]. This is because, unlike a standard optimal control problem where the theoretical issue of existence of a solution can be practically supplanted by engineering judgment, a Riemann–Stieltjes control defies intuition in that closed-loop-like performance can be obtained using open-loop controls. Furthermore, it is very easy to formulate a specific problem RS with no solution [8]. Thus, a Riemann–Stieltjes optimal control problem inherits all the theoretical difficulties of a standard optimal control problem while making its practical computation even more challenging. Thus, a vast number of open problems and opportunities remain to be explored.

VIII. Conclusions

The Riemann–Stieltjes optimal control problem offers a mathematical framework to address a new kind of practical optimality based on uncertainties in the various parameters of the system under consideration. It is extremely challenging to even write a closed-form expression for the Riemann–Stieltjes extremal control because it requires an analytical solution to the Hamiltonian integral before a minimization can be performed. The computational problem is also daunting but is more tractable through the use of hyperpseudospectral methods. Ground test results at Honeywell showed

that an offline computed Riemann–Stieltjes optimal control is immediately implementable online. This implies that nearly all of the computational burden for flight implementation can be transferred to the ground. Because the scope of a Riemann–Stieltjes optimal control problem is fairly large, and its flight applications quite immediate, rapid advances in both theory and computation are expected to follow in the coming years.

Acknowledgments

We thank R. S. Erwin at the U.S. Air Force Research Laboratory (AFRL) for making the miniature momentum control system hardware available as part of the AFRL guest investigator program, and B. Hamilton at Honeywell for his help in implementing the ground test runs on the momentum control systems testbed. We also thank the Judge Advocate General's office for their encouragement and strong support in filing our application for the U.S. patent 14/081,921.

References

- [1] Kolmogorov, A. N., and Fomin, S. V., *Elements of the Theory of Functions and Functional Analysis*, Dover, New York, 1999.
- [2] Phillips, E. R., *Introduction to Analysis and Integration Theory*, Dover, New York, 1984.
- [3] Longuski, J. M., Guzmán, J. S. J., and Prussing, J. E., *Optimal Control with Aerospace Applications*, Springer–Verlag, New York, 2014, pp. 19–38, Chap. 2.
- [4] Vinter, R. B., *Optimal Control*, Birkhäuser, Boston, 2000, pp. 1–60, 201–228, 321–359, 397–432, 435–487, Chaps. 1, 6, 9, 11, 12.
- [5] Clarke, F. H., Ledyaev, Y. S., Stern, R. J., and Wolenski, P. R., *Nonsmooth Analysis and Control Theory*, Springer–Verlag, New York, 1998, pp. 177–256, Chap. 4.
- [6] Ross, I. M., *A Primer on Pontryagin's Principle in Optimal Control*, Collegiate, San Francisco, 2009, pp. 19–38, Chap. 2.
- [7] Kurzhanski, A. B., and Filippova, T. F., “On the Theory of Trajectory Tubes—A Mathematical Formalism for Uncertain Dynamics, Viability and Control,” *Advances in Nonlinear Dynamics and Control: A Report from Russia*, Birkhäuser, Boston, 1993, pp. 122–188.
- [8] Ross, I. M., Proulx, R. J., and Karpenko, M., “Unscented Optimal Control for Space Flight,” *24th International Symposium on Space Flight Dynamics (ISSFD)*, John Hopkins Univ. Applied Physics Lab., Laurel, MD, May 2014, http://issfd.org/ISSFD_2014/ISSFD24_Paper_S12-5_Karpenko.pdf [retrieved 2 July 2014].
- [9] Ross, I. M., Proulx, R. J., and Karpenko, M., “Unscented Optimal Control for Orbital and Proximity Operations in an Uncertain Environment: A New Zermelo Problem,” *Proceedings of the AIAA/AAS Astrodynamics Specialist Conference*, AIAA Paper 2014-4423, Aug. 2014.
- [10] Malefaki, S., and Iliopoulos, G., “Simulation from a Target Distribution Based on Discretization and Weighting,” *Communications in Statistics — Simulation and Computation*, Vol. 38, No. 4, 2009, pp. 829–845. doi:10.1080/03610910802657904
- [11] Ross, I. M., “A Roadmap for Optimal Control: The Right Way to Commute,” *Annals of the New York Academy of Sciences*, Vol. 1065, No. 1, 2005, pp. 210–231. doi:10.1196/annals.1370.015
- [12] Ross, I. M., and Karpenko, M., “A Review of Pseudospectral Optimal Control: From Theory to Flight,” *Annual Reviews in Control*, Vol. 36, No. 2, 2012, pp. 182–197. doi:10.1016/j.arcontrol.2012.09.002
- [13] Gong, Q., Ross, I. M., and Fahroo, F., “Costate Computation by a Chebyshev Pseudospectral Method,” *Journal of Guidance, Control, and Dynamics*, Vol. 33, No. 2, 2010, pp. 623–628. doi:10.2514/1.45154
- [14] Gong, Q., Ross, I. M., Kang, W., and Fahroo, F., “Connections Between the Covector Mapping Theorem and Convergence of Pseudospectral Methods for Optimal Control,” *Computational Optimization and Applications*, Vol. 41, No. 3, 2008, pp. 307–335. doi:10.1007/s10589-007-9102-4
- [15] Vinter, R. B., “Minimax Optimal Control,” *SIAM Journal on Control and Optimization*, Vol. 44, No. 3, 2005, pp. 939–968. doi:10.1137/S0363012902415244
- [16] Boltyanski, V. G., and Poznyak, A. S., *Robust Maximum Principle: Theory and Applications*, Birkhäuser, New York, 2012, pp. 269–283, Chap. 11.
- [17] Trefethen, L. N., *Spectral Methods in MATLAB*, Soc. for Industrial and Applied Mathematics, Philadelphia, 2000.

- [18] Boyd, J., *Chebyshev and Fourier Spectral Methods*, Dover, Minola, NY, 2001.
- [19] Williams, P., "Jacobi Pseudospectral Method for Solving Optimal Control Problems," *Journal of Guidance, Control, and Dynamics*, Vol. 27, No. 2, 2004, pp. 293–297.
doi:10.2514/1.4063
- [20] Gong, Q., Ross, I. M., and Fahroo, F., "Pseudospectral Optimal Control on Arbitrary Grids," *Proceedings of the AAS/AIAA Astrodynamics Specialist Conference*, American Astronautical Soc. Paper 2009-405, Pittsburgh, PA, 2009; also *Advances in the Astronautical Sciences*, Vol. 135, 2009, pp. 103–116.
- [21] Gong, Q., Fahroo, F., and Ross, I. M., "Spectral Algorithm for Pseudospectral Methods in Optimal Control," *Journal of Guidance, Control, and Dynamics*, Vol. 31, No. 3, 2008, pp. 460–471.
doi:10.2514/1.32908
- [22] Fahroo, F., and Ross, I. M., "Pseudospectral Methods for Infinite-Horizon Nonlinear Optimal Control Problems," *Journal of Guidance, Control, and Dynamics*, Vol. 31, No. 4, 2008, pp. 927–936.
doi:10.2514/1.33117
- [23] Fahroo, F., and Ross, I. M., "Advances in Pseudospectral Methods for Optimal Control," *AIAA Guidance, Navigation, and Control Conference*, AIAA Paper 2008-7309, 2008.
- [24] Kang, W., Ross, I. M., and Gong, Q., "Pseudospectral Optimal Control and Its Convergence Theorems," *Analysis and Design of Nonlinear Control Systems*, Springer-Verlag, Berlin, 2008, pp. 109–126.
- [25] Kang, W., "Rate of Convergence for the Legendre Pseudospectral Optimal Control of Feedback Linearizable Systems," *Journal of Control Theory and Applications*, Vol. 8, No. 4, 2010, pp. 391–405.
doi:10.1007/s11768-010-9104-0
- [26] Fahroo, F., and Ross, I. M., "Convergence of the Costates Does Not Imply Convergence of the Control," *Journal of Guidance, Control, and Dynamics*, Vol. 31, No. 5, 2008, pp. 1492–1497.
doi:10.2514/1.37331
- [27] Kang, W., Gong, Q., and Ross, I. M., "On the Convergence of Nonlinear Optimal Control Using Pseudospectral Methods for Feedback Linearizable Systems," *International Journal of Robust and Nonlinear Control*, Vol. 17, No. 14, 2007, pp. 1251–1277.
doi:10.1002/(ISSN)1099-1239
- [28] Cools, R., Mysovskikh, I. P., and Schmid, H. J., "Cubature Formulae and Orthogonal Polynomials," *Journal of Computational and Applied Mathematics*, Vol. 127, Nos. 1–2, 2001, pp. 121–152.
doi:10.1016/S0377-0427(00)00495-7
- [29] Engels, H., *Numerical Quadrature and Cubature*, Academic Press, New York, 1980.
- [30] Proulx, R., Ross, I. M., and Karpenko, M., "Method and Apparatus for State Space Trajectory Control of Uncertain Dynamical Systems," U.S. Patent 14/081,921, filed 15 Nov. 2013.
- [31] Julier, S. J., and Uhlmann, J. K., "New Extension of the Kalman Filter to Nonlinear Systems," *Proceedings of SPIE 3068: Signal Processing, Sensor Fusion, and Target Recognition VI*, Vol. 3068, July 1997, pp. 182–193.
doi:10.1117/12.280797
- [32] Julier, S. J., Uhlmann, J. K., and Durrant-Whyte, H. F., "A New Approach for Filtering Nonlinear Systems," *Proceedings of the 1995 American Control Conference*, Vol. 3, IEEE Publ., Piscataway, NJ, 1995, pp. 1628–1632.
doi:10.1109/ACC.1995.529783
- [33] Ross, I. M., and D'Souza, C. D., "Hybrid Optimal Control Framework for Mission Planning," *Journal of Guidance, Control, and Dynamics*, Vol. 28, No. 4, July–Aug. 2005, pp. 686–697.
doi:10.2514/1.8285
- [34] Cordeau, J.-F., and Laporte, G., "Maximizing the Value of an Earth Observation Satellite Orbit," *Journal of the Operational Research Society*, Vol. 56, No. 8, 2005, pp. 962–968.
doi:10.1057/palgrave.jors.2601926
- [35] Mansour, M. A. A., and Dessouky, M. M., "Genetic Algorithm Approach for Solving the Daily Photography Selection Problem of the SPOT5 Satellite," *Computers and Industrial Engineering*, Vol. 58, No. 3, 2010, pp. 509–520.
doi:10.1016/j.cie.2009.11.012
- [36] Karpenko, M., Bhatt, S., Bedrossian, N., and Ross, I. M., "Design and Flight Implementation of Operationally Relevant Time-Optimal Spacecraft Maneuvers," *Proceedings of the AAS/AIAA Astrodynamics Specialist Conference*, American Astronautical Soc. Paper 2011-586, Girdwood, AK, July–Aug. 2011.
- [37] Karpenko, M., Bhatt, S., Bedrossian, N., and Ross, I. M., "Flight Implementation of Shortest-Time Maneuvers for Imaging Satellites," *Journal of Guidance, Control, and Dynamics*, Vol. 37, No. 4, 2014, pp. 1069–1079.
doi:10.2514/1.62867
- [38] Wie, B., *Space Vehicle Dynamics and Control*, AIAA, Reston, VA, 1998, pp. 331–462, Chaps. 6, 7.
- [39] Kurokawa, H., Yajima, N., and Usui, S., "New Steering Law of a Single-Gimbal CMG System of Pyramid Configuration," *Proceedings of the Xth IFAC Symposium on Automatic Control in Space*, Pergamon Press, Oxford, June 1985, pp. 249–255.
- [40] Ross, I. M., *Beginner's Guide to DIDO: A MATLAB Application Package for Solving Optimal Control Problems*, Elissar Global, Carmel, CA, Nov. 2007.
- [41] Kushner, H. J., "Necessary Conditions for Continuous Parameter Stochastic Optimization Problems," *SIAM Journal on Control and Optimization*, Vol. 10, No. 3, 1972, pp. 550–565.
doi:10.1137/0310041
- [42] Peng, S., "General Stochastic Maximum Principle for Optimal Control Problems," *SIAM Journal on Control and Optimization*, Vol. 28, No. 4, 1990, pp. 966–979.
doi:10.1137/0328054
- [43] Fleming, W. H., and Rishel, R. W., *Optimal Deterministic and Stochastic Control*, Springer-Verlag, Berlin, 1975.
- [44] Aubin, J.-P., Bayen, A. M., and Saint-Pierre, P., *Viability Theory: New Directions*, 2nd ed., Springer-Verlag, Berlin, 2011.
- [45] Aubin, J.-P., Chen, L., Dordan, O., Faleh, A., Lezan, G., and Planchet, F., "Stochastic and Tychastic Approaches to Guaranteed ALM Problem," *Bulletin Français d'Actuariat*, Vol. 12, No. 23, 2012, pp. 59–95.
- [46] Clarke, F. H., *Optimization and Nonsmooth Analysis*, Wiley, New York, 1983, pp. 1–23, Chap. 1.
- [47] Aubin, J.-P., "Viability Kernels and Capture Basins of Sets Under Differential Inclusions," *SIAM Journal on Control and Optimization*, Vol. 40, No. 3, 2001, pp. 853–881.
doi:10.1137/S036301290036968X
- [48] Lygeros, J., "On Reachability and Minimum Cost Optimal Control," *Automatica*, Vol. 40, No. 6, 2004, pp. 917–927.
doi:10.1016/j.automatica.2004.01.012
- [49] Aubin, J.-P., *Viability Theory*, Birkhäuser, Boston, 1991.
- [50] Aubin, J.-P., "Tychastic Viability: A Mathematical Approach to Time and Uncertainty," *Acta Biotheoretica*, Vol. 61, No. 3, 2013, pp. 329–340.
doi:10.1007/s10441-013-9194-4
- [51] Koopman, B. O., "Theory of Search, I: Target Detection," *Operations Research*, Vol. 4, No. 5, 1956, pp. 503–531.
doi:10.1287/opre.4.5.503
- [52] Ohsumi, A., "Optimal Search for a Markovian Target," *Naval Research Logistics*, Vol. 38, No. 4, pp. 531–554, 1991.
doi:10.1002/(ISSN)1520-6750
- [53] Li, J.-S., "Ensemble Control of Finite-Dimensional Time-Varying Linear Systems," *IEEE Transactions on Automatic Control*, Vol. 56, No. 2, 2011, pp. 345–357.
doi:10.1109/TAC.2010.2060259
- [54] Seywald, H., and Kumar, R. R., "Desensitized Optimal Trajectories," *Advances in Astronautical Sciences*, Vol. 93, Feb. 1996, pp. 103–116; also American Astronautical Soc. Paper 1996-107, 1996.
- [55] Darlington, J., Pantelides, C. C., Rustem, B., and Tanyi, B. A., "Decreasing the Sensitivity of Open-Loop Optimal Solutions in Decision Making Under Uncertainty," *European Journal of Operational Research*, Vol. 121, No. 2, 2000, pp. 343–362.
doi:10.1016/S0377-2217(99)00034-X
- [56] Hover, F. S., and Triantafyllou, M. S., "Gradient Dynamic Optimization with Legendre Chaos," *Automatica*, Vol. 44, No. 1, 2008, pp. 135–140.
doi:10.1016/j.automatica.2007.06.001
- [57] Fisher, J., and Bhattacharya, R., "Optimal Trajectory Generation with Probabilistic System Uncertainty Using Polynomial Chaos," *Journal of Dynamic Systems, Measurement, and Control*, Vol. 133, No. 1, Jan. 2011, Paper 014501.
doi:10.1115/1.4002705
- [58] Ghosh, P., and Conway, B., "Near-Optimal Feedback Strategies Synthesized Using a Spatial Statistical Approach," *Journal of Guidance, Control, and Dynamics*, Vol. 36, No. 4, 2013, pp. 905–919.
doi:10.2514/1.59568
- [59] Washburn, A. R., *Search and Detection*, 4th ed., Informa, Linthicum, MD, 2002.
- [60] Phelps, C., Gong, Q., Royset, J. O., and Kaminer, I., "Consistent Approximation of an Optimal Search Problem," *Automatica*, Vol. 50, No. 12, 2014, pp. 2987–2997.
- [61] Phelps, C., Royset, J. O., and Gong, Q., "Sample Average Approximations in Optimal Control of Uncertain Systems," *Proceedings of the 52nd IEEE Conference on Decision and Control*, IEEE Publ.,

- Piscataway, NJ, 2013, pp. 1958–1965.
doi:10.1109/CDC.2013.6760168
- [62] Brif, C., Chakrabarti, R., and Rabitz, H., “Control of Quantum Phenomena: Past, Present and Future,” *New Journal of Physics*, Vol. 12, No. 7, 2010, Paper 075008.
doi:10.1088/1367-2630/12/7/075008
- [63] Li, J.-S., and Khaneja, N., “Control of Inhomogeneous Quantum Ensembles,” *Physical Review A: General Physics*, Vol. 73, No. 3(R), 2006, Paper 030302.
doi:10.1103/PhysRevA.73.030302
- [64] Li, J.-S., Ruths, J., Yu, T.-Y., Arthanari, H., and Wagner, G., “Optimal Pulse Design in Quantum Control: A Unified Computational Method,” *Proceedings of the National Academy of Sciences*, Vol. 108, No. 5, Feb. 2011, pp. 1879–1884.
doi:10.1073/pnas.1009797108